

UNCLASSIFIED
CONFIDENTIAL

RM A55J24

NACA RM A55J24



RESEARCH MEMORANDUM

AN EXPERIMENTAL INVESTIGATION OF THE HINGE-MOMENT
CHARACTERISTICS OF A CONSTANT-CHORD CONTROL
SURFACE OSCILLATING AT HIGH FREQUENCY

By David E. Reese, Jr., and William C. A. Carlson

Ames Aeronautical Laboratory
Moffett Field, Calif.

TECHNICAL LIBRARY
AIRSEARCH MANUFACTURING CO.
9851-9951 SEPULVEDA BLVD.
LOS ANGELES 45
CALIFORNIA

CLASSIFIED DOCUMENT

This material contains information affecting the National Defense of the United States within the meaning of the espionage laws, Title 18, U.S.C., Secs. 793 and 794, the transmission or revelation of which in any manner to an unauthorized person is prohibited by law.

NATIONAL ADVISORY COMMITTEE FOR AERONAUTICS

WASHINGTON

December 28, 1955

CONFIDENTIAL
UNCLASSIFIED

CANCELLED

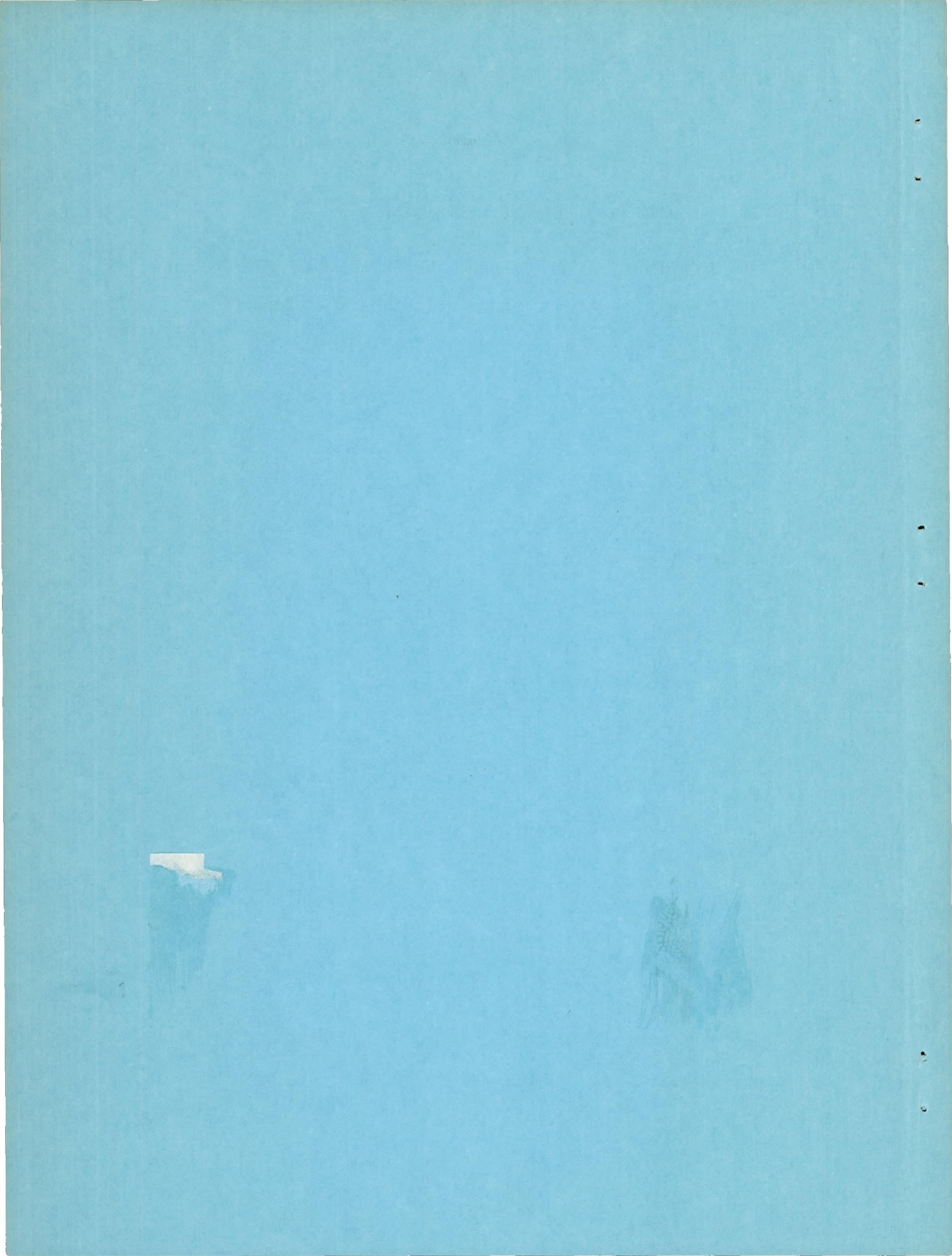
Classification

CHANGED TO

By authority of *MR. F. T. [unclear]* 7/14/60

Changed by *KEA* Date *7-5-60*

Uncl. [unclear]



NATIONAL ADVISORY COMMITTEE FOR AERONAUTICS

RESEARCH MEMORANDUMAN EXPERIMENTAL INVESTIGATION OF THE HINGE-MOMENT
CHARACTERISTICS OF A CONSTANT-CHORD CONTROL
SURFACE OSCILLATING AT HIGH FREQUENCY

By David E. Reese, Jr., and William C. A. Carlson

SUMMARY

The results of an experimental investigation of the hinge-moment characteristics of a constant-chord control surface oscillating at high frequency are presented. The control surface was mounted on an aspect-ratio-2 triangular wing. The aerodynamic restoring-moment coefficient and damping-moment coefficient were determined at a frequency of 260 cycles per second for a Mach number range of 0.6 to 0.8 and 1.3 to 1.9 at angles of attack of 5° and 10° .

The test results showed linear theory to be a reliable guide to the prediction of the trend of the restoring-moment coefficient with Mach number for the supersonic speed range of the investigation but overestimated the magnitude of the coefficient. The experimental values of the damping-moment coefficient were, for the most part, more positive than those indicated by the theory and, for some conditions, could lead to instability of the control surface. Comparison of the results of this investigation with those of previous investigations at 0 and 50 cycles per second showed that frequency had little effect on the restoring-moment coefficient. The damping-moment coefficient was similarly insensitive to frequency at an oscillation amplitude of $\pm 1.0^\circ$ but at an amplitude of $\pm 2.5^\circ$ the results showed a destabilizing shift with increasing frequency.

INTRODUCTION

A major factor in the design of servo-driven control systems for aircraft is the evaluation of the static and dynamic hinge moments acting on the controls. A considerable amount of effort has been put into the evaluation of the static moments in both theoretical and experimental

investigations. However, a very limited amount of information is available on the dynamic hinge moments of finite-span controls at transonic and supersonic speeds.

One facet of this problem that has received little attention is the effect of frequency on the dynamic hinge moments. The higher natural frequency of the controls resulting from the increase in aerodynamic restoring moment at supersonic speeds has put additional emphasis on the need for evaluating dynamic hinge moments at high frequencies. A recent unpublished theoretical study of the air forces on an oscillating unswept rectangular control surface at supersonic speeds made by Julian H. Berman of the Langley Laboratory includes the effects of frequency up to the fifth power in reduced frequency. In reference 1, experimental data for an oscillating constant-chord control surface on a triangular wing are presented for low values of reduced frequency. The present investigation was designed to extend those results to higher reduced frequencies.

SYMBOLS

C_h	hinge-moment coefficient, $\frac{\text{hinge moment}}{\frac{1}{2}\rho V^2 S c}$
$C_{h\delta}$	aerodynamic restoring-moment coefficient, $\frac{\partial C_h}{\partial \delta}$
$C_{h\dot{\delta}}$	aerodynamic damping-moment coefficient, $\frac{\partial C_h}{\partial \left(\frac{\dot{\delta} c}{2V}\right)}$
I	mass moment of inertia of the oscillating system, ft-lb-sec ²
K	restoring moment per unit deflection, ft-lb
M	Mach number, $\frac{V}{\text{speed of sound}}$
S	control-surface area, sq ft
V	velocity of air stream, ft/sec
c	control-surface chord, ft
f	frequency, cps
k	reduced frequency, $\frac{\omega c}{2V}$
t	time, sec

- α angle of attack, deg
- δ control-surface deflection angle, radians except where noted
- μ damping moment per unit angular velocity, ft-lb-sec
- ρ density of air stream, $\frac{\text{lb-sec}^2}{\text{ft}^4}$
- ω angular frequency, $2\pi f$, radians/sec

Subscripts

- a aerodynamic
- o wind off or tare
- T total

APPARATUS

Wind Tunnel

The model was tested in the Ames 6- by 6-foot supersonic wind tunnel which is of the closed-return, variable-density type and which has a Mach number range of 0.6 to 0.9 and 1.2 to 1.9. A detailed description of the flow characteristics of this wind tunnel can be found in reference 2.

Model

The model used in this investigation consisted of an aspect-ratio-2 triangular wing in combination with a slender body of revolution. The wing had NACA 0005 sections in streamwise planes. The dimensions of the wing-fuselage combination are given in figure 1. One wing panel was fitted with a constant-chord control surface with an area equal to 15.2 percent of the exposed area of the wing panel. The control surface was fastened to the wing by means of a flat spring running the full length of the control-surface leading edge. This spring mounting placed the effective hinge line of control surface deflections at the leading edge of the control. The model was constructed of steel with the exception of the control surface which was fabricated from magnesium to keep its mass small. As a safety measure, a solenoid-operated locking mechanism was provided to prevent any damage to the control surface if flutter were encountered. A photograph of the model is shown in figure 2.

Drive System

As was stated in the Introduction, the primary purpose of this investigation was to extend the work of reference 1 to higher values of reduced frequency. It was felt that a resonant system afforded the best possibility of achieving a high frequency of oscillation and, as a consequence, a drive system supplying an oscillating torque was indicated rather than the fixed-amplitude drive described in reference 1. It was found that a torque motor, a device developed in recent years primarily for high-speed actuation of hydraulic valves, would be satisfactory as a drive motor for the model of this investigation. A brief description of the design and construction of this motor is given in the appendix.

The manner in which the motor was mounted in the model is shown in figure 3. Since it was necessary to keep the natural frequency of the armature-control-surface combination high, a spring was added in the form of crossed flexures. The flexures also provided a means for indicating the amplitude of the control-surface motion. A strain-gage bridge was mounted on one of the flexures and its output was amplified and fed into a recording oscillograph. The deflection recorded by the oscillograph was then calibrated as a function of control-surface deflection.

It was originally intended to drive the control surface at the resonant frequency of the system and measure the current in the armature of the torque motor necessary to sustain a given amplitude of oscillation. This current would be proportional to the torque output of the motor. If the oscillating system can be adequately described by a single-degree-of-freedom equation of motion, the torque at resonance is directly proportional to the damping of the system. Thus the damping of the control surface could be calculated from the armature current of the torque motor. In practice, however, it was found that consistent results could not be obtained using this method. The primary reason for this lack of consistency appeared to be due to a small amount of play in the connection between the torque-motor armature and the control surface which absorbed an unknown amount of the torque output of the motor. In addition, the drive frequency was set manually and some error could have appeared if the drive frequency did not coincide with the resonant frequency.

Further bench tests showed that consistent data could be obtained through the use of the free-oscillation technique. In this method, the system was driven at its resonant frequency up to a given amplitude. The armature circuit of the torque motor was then opened and the resulting free oscillation was recorded. The damping of the system was then obtained from the decrement in the usual manner. In this approach, the torque motor provided the exciting power to drive the control surface to the oscillation amplitude at which the free oscillation was to start. For tests where the stiffness of the surface to be oscillated is much larger than that of the restraining spring, the same result can be accomplished with an impulsive

deflection of the surface to the desired amplitude. When a high frequency of oscillation is desired, however, the stiffness of the spring can be of the same order of magnitude as the torsional stiffness of the surface. An attempt to produce an impulsive deflection of the surface would then lead to a distortion of the surface. In the present system, the spring stiffness was distributed along the leading edge of the control. At resonance the spring torque was just balanced by the inertia torque at each point along the span of the control. Thus the only torque required to deflect the control was that necessary to overcome the damping of the system which was, in turn, too small to deform the control surface.

TESTS

The investigation of the oscillatory hinge-moment characteristics of the control surface was conducted over a Mach number range of 0.6 to 0.8 and 1.3 to 1.9 at a Reynolds number of 3.1×10^6 based on the wing mean aerodynamic chord. Data were obtained at angles of attack of 0° , 5° , and 10° . The wind-on frequency of oscillations was approximately 260 cycles per second.

Reduction of Data

As pointed out earlier, the free-oscillation technique was used to obtain the data for this investigation. The differential equation describing the damped free oscillations of a single-degree-of-freedom motion is

$$I\ddot{\delta} + \mu_T\dot{\delta} + K_T\delta = 0 \quad (1)$$

The total damping moment can be written $\mu_T\dot{\delta} = (\mu_O + \mu_a)\dot{\delta}$.¹ The total restoring moment can be expressed, in turn, as $K_T\delta = (K_O + K_a)\delta$. The expression for the aerodynamic damping-moment coefficient is then

¹It should be noted that this statement is true only if μ_O is not affected by the frequency change associated with wind-on oscillations. The frequency change for this investigation was never greater than 4 percent of the wind-off frequency. Calculations based on a linear variation of tare damping with frequency showed that neglecting this frequency change would introduce an error smaller than the uncertainty due to random errors described in the section "Precision of Data."

$$C_{h\dot{\delta}} = - \frac{(\mu_T - \mu_O) \dot{\delta}}{\frac{1}{2} \rho V^2 S c \left(\frac{\dot{\delta} c}{2V} \right)} = - \frac{4(\mu_T - \mu_O)}{\rho V S c^2} \quad (2)$$

and that for the aerodynamic restoring-moment coefficient is

$$C_{h\delta} = \frac{(K_T - K_O) \delta}{\frac{1}{2} \rho V^2 S c \delta} = \frac{2(K_T - K_O)}{\rho V^2 S c} \quad (3)$$

Thus, aside from the quantities pertaining to the flow conditions and model geometry, the quantities necessary for calculation of these two coefficients are μ_T , μ_O , K_T , and K_O .

If in equation (1) the initial conditions $\delta = \delta_{\max}$ and $\dot{\delta} = 0$ at $t = 0$ are chosen, the solution to the equation may be written as

$$\delta = \delta_{\max} e^{-\frac{\mu_T}{2I} t} \left(\cos \omega t + \frac{\mu_T}{2I} \sin \omega t \right) \quad (4)$$

where

$$\omega = \sqrt{\frac{K_T}{I} - \left(\frac{\mu_T}{2I} \right)^2} \quad (5)$$

The envelope of the curve described by equation (4) is given by

$$\delta = \delta_{\max} e^{-\frac{\mu_T}{2I} t} \quad (6)$$

From equation (6) it can be shown that

$$\mu_T = \frac{2I}{\Delta t} \ln \frac{\delta_1}{\delta_2} \quad (7)$$

where

δ_1 amplitude of the envelope curve at t_1

δ_2 amplitude of the envelope curve at t_2

Δt $t_2 - t_1$

One of the assumptions implicit in the solution of the differential equation above is that the coefficients in equation (1) are constants. It was found, however, that apparent nonlinearities in the mechanical system resulted in a variation of μ_0 with amplitude. Since this was true, then strictly speaking, the expressions given in equations (4), (5), (6), and (7) were not valid. However, the motion represented by equation (1) for nonconstant coefficients can be divided into several intervals in time and an approximate solution can be obtained which assumes constant coefficients in each of the time intervals.

For the reduction of the data obtained in this investigation, the amplitude of the envelope curve was measured every 1/60th of a second. The damping parameter, μ_T , was calculated for each time interval using equation (7). This was done for each of the five oscillation records obtained at each test condition. The values of the damping parameter were then plotted as a function of amplitude. The resulting plots showed that μ_T was approximately a linear function of amplitude but that there was some scatter in the points defining this linear relationship. In order to get a representative value of μ_T to use in the calculations of the damping coefficient, a straight line was fitted to the points obtained from all five of the oscillation records using the method of least squares. This straight line was then used to calculate the value of μ_T at a given amplitude of oscillation.

The tare damping μ_0 for the system was obtained by taking wind-off oscillation records at several pressures from 15 to 3 pounds per square inch absolute as the wind tunnel was evacuated. The values of μ_0 for a given amplitude of oscillation obtained from these records were then plotted as a function of pressure. These data were extrapolated to zero pressure to obtain the true value of μ_0 at that amplitude.

The frequency of the wind-off oscillations along with the value of K_0 obtained from static calibration were used to calculate the moment of inertia of the moving parts of the mechanical system. It was found that, for all conditions encountered during the investigation, the value of $(\mu_T/2I)^2$ was small relative to K_T/I so that equation (5) could be simplified to

$$\omega = \sqrt{\frac{K_T}{I}} \quad (8)$$

Thus for wind-off conditions

$$I = \frac{K_0}{4\pi^2 f^2} \quad (9)$$

The moment of inertia of the system and the wind-on frequency of oscillation being known, equation (8) was then used to find the value of K_T .

It should be noted that both the wind-off and wind-on frequencies were determined by counting the number of cycles in a given time interval on the oscillograph record. In most cases the time interval covered the greater part of the duration of the model oscillations so that the calculated frequency was actually an average frequency for the transient. As a result, the values of the aerodynamic restoring-moment coefficient calculated from these frequencies represent average values for the range of oscillation amplitudes up to 2.5° . An attempt was made to determine the effect of amplitude on C_{h_0} by measuring the frequency over small portions of the decrement curve. The use of a shorter time interval in the determination of the frequency resulted in enough scatter in the data to obscure any amplitude effects that might have been present.

Corrections to Data

No wind-tunnel-wall corrections were made to the hinge-moment coefficients presented in this report. Some information is available on the effect of tunnel walls on the forces and moments acting on an oscillating wing in subsonic two-dimensional flow (refs. 3 and 4) but no published results concerned with this problem related to a finite wing are known to exist. However, the tunnel resonance phenomenon mentioned in references 3 and 4 can be used to give an indication of possible tunnel-wall effects on a finite-span model. The values of the fundamental tunnel resonant frequency for a closed rectangular tunnel were computed using the expression given by Woolston and Runyan in reference 4. It was found that the frequency of oscillation of the control surface was from 5.0 to 6.8 times the fundamental tunnel resonant frequency, depending on the Mach number. While the theory admits the possibility of higher harmonics of the resonant frequency at 5 and 7 times the fundamental frequency, it also shows that the effect on the forces on the model are restricted to a small frequency range near the critical frequency if the ratio of tunnel height to wing chord is large. Since the ratio of tunnel height to control-surface chord was relatively large for this investigation, only the results obtained when the oscillation frequency was 5 times the fundamental resonant frequency ($M = 0.6$) would be in question. But the data obtained at this Mach number do not appear to be out of line with the remainder of the data obtained at subsonic speeds, so it is felt that tunnel resonance effects were probably small.

Precision of Data

It was noted previously that the values of μ and K , in addition to the density and velocity of the flow, must be determined to permit the calculation of the hinge-moment coefficients for the control surface. The precision of the data will be limited then by the accuracy of the various factors involved in their computation.

As has been shown, the values of μ_T and μ_O used in the calculations for the damping coefficients were computed from the equations for straight lines that were fitted to the experimental data. The scatter of the data about those lines is then a measure of the uncertainty in the determination of μ_T and μ_O . This uncertainty was taken to be the standard deviation of the experimental values from the straight lines. These calculations led to an uncertainty of $\pm 5.7 \times 10^{-5}$ ft-lb-sec for μ_O and the values of μ_T obtained at supersonic speeds. The uncertainty in μ_T at subsonic Mach numbers was $\pm 2.2 \times 10^{-4}$ ft-lb-sec. For comparison purposes, a representative value of μ_O used in the reduction of the data was 1.2×10^{-3} ft-lb-sec while typical values of μ_T obtained at subsonic and supersonic speeds were 2.8×10^{-3} and 1.0×10^{-3} ft-lb-sec, respectively.

The uncertainty in the value of the total spring constant K_T was determined by the accuracy with which the wind-on frequency could be measured. The standard deviation of the frequency for subsonic speeds was approximately equal to that for supersonic speeds and led to an uncertainty in K_T of ± 0.58 ft-lb/radian as compared to a typical value of K_T obtained during the investigation of 140 ft-lb/radian. The mechanical spring constant K_O was determined from static calibrations and had a value of 134 ft-lb/radian. The uncertainty of several calibrations was ± 1.4 ft-lb/radian.

The calculation of the density and velocity of the flow was based on measured values of the tunnel stagnation temperature and pressure. The least readings of the instruments measuring these quantities were 2° F and 0.2 centimeters of mercury, respectively, and led to an uncertainty in the density of $\pm 7.9 \times 10^{-5}$ lb/cu ft and in velocity of ± 5.2 ft/sec.

The total uncertainties in the hinge-moment coefficients were taken to be the square root of the sum of the squares of the effects of the uncertainties given above. These calculations gave values for Ch_δ of ± 0.58 for subsonic speeds and ± 0.20 for supersonic speeds. The uncertainty in Ch_δ was ± 0.20 for both subsonic and supersonic Mach numbers.

The discussion above is concerned with the effect of random errors on the results. Systematic errors must also be considered. The primary source of systematic errors for this investigation lay in the evaluation of the tare damping and mechanical spring constant. The values given above show that the tare damping was, on the average, about six times

the aerodynamic damping for the supersonic speed range and that the mechanical spring constant was about twenty times the aerodynamic spring constant. Thus any change in these quantities from wind-off to wind-on conditions could introduce appreciable errors in the calculated values of the aerodynamic damping and restoring moments. An evaluation of the change in tare damping and mechanical spring constant with aerodynamic load is very difficult. Since the aerodynamic loads on the control surface were small, however, they probably had little effect on these quantities. The forces on the wing were, of course, much larger. However, the fact that the data obtained at angles of attack of 5° and 10° show little change even though the forces on the wing change by a factor of 2 makes it appear that this effect was also small. While these general considerations indicate that the effect of aerodynamic loads on the tare damping and mechanical spring constant were probably small, no specific conclusions can be drawn and the possibility of some effects must be admitted.

RESULTS AND DISCUSSION

Theory

The theoretical values for the restoring-moment and damping-moment coefficients presented in this report were calculated for the supersonic speed range using the results of an unpublished analysis by Julian H. Berman of the Langley Laboratory. In this analysis, Berman has derived the velocity potential for the rotating aileron as a power series in terms of a frequency parameter. The approach used was the same as that used by Nelson, Rainey, and Watkins (ref. 5) in which the Laplace transformation was used to obtain the potential in the form of a definite integral. The integrand of this integral was then expanded in powers of the frequency of oscillation and integrated term by term. Berman carried this expansion out to the fifth power of the frequency. The values for the forces and moments on the control surface were then obtained from the potential in the usual manner.

The control surface considered by Berman was rectangular in plan form and was mounted on a rectangular wing. The outboard edge of the control was taken to be coincident with the side edge of the wing. The inboard edge was treated as if there were a diaphragm sealing the gap between the wing and the control, thereby preventing any flow between the upper and lower surfaces at this edge. It should be pointed out that, while Berman's analysis was concerned with a rectangular control surface mounted on a rectangular wing, the wing has no effect on the forces due to the control motion in supersonic flow. Thus the analysis is applicable to a rectangular control on any wing, provided the control leading edge is perpendicular to the free-stream direction.

It is evident that although the theory was developed for a rectangular control surface, the plan form of the control of the present investigation was trapezoidal. It was felt, however, that the effect of the raked tip would be small, particularly at the higher Mach numbers.

A theoretical solution for the finite control oscillating in subsonic compressible flow has not been obtained and little information is available for the infinite span control. For this reason, no comparison has been made with theory for subsonic speeds.

Experiment

The results of the experimental investigation of the hinge-moment characteristics of the control surface are presented in figures 4 through 7. Figure 4 shows the effect of angle of attack on the aerodynamic restoring-moment coefficient for this investigation. Figure 5 compares part of these results with their corresponding values from references 1 and 6 in order to show the effects of frequency on the restoring-moment coefficient. Figure 6 presents the effect of angle of attack on the damping-moment coefficient for this investigation while figure 7 compares part of these data with corresponding data from reference 1, again to show the effects of frequency.

It will be noted that the data for $\alpha = 0^\circ$ have not been presented. It was discovered after the investigation had been completed that play in the support system had introduced serious errors into the results obtained at $\alpha = 0^\circ$ and for this reason they have been omitted. At angles of attack of 5° and 10° the lift loads on the wing removed this play and the data obtained under these conditions are correct within the limits given in the section "Precision of Data."

Restoring moments.- In figure 4 the aerodynamic restoring-moment coefficient is plotted against Mach number for angles of attack of 5° and 10° . The experimental results show the effects of angle of attack to be negligible for the range of this investigation for both subsonic and supersonic speeds. The figure also shows Berman's analysis to be a reliable guide for the prediction of the trends of the data with Mach number but that it overestimated the magnitude of the coefficient by as much as 50 percent at the low supersonic Mach numbers.

One possible explanation for this lack of agreement between theory and experiment is that the assumption of zero thickness on which the theory was based is not valid. In reference 7 an expression is given for the hinge moment due to δ , including second-order thickness effects. This expression is valid only for two-dimensional wing-control-surface combinations, however. In order to apply these results to the present theory, a correction factor was calculated by dividing the second-order

expression by the usual first-order result. The theoretical values for $C_{h\delta}$ calculated from Berman's analysis were then multiplied by this factor to give an approximate theoretical result for a finite-span wing-control-surface combination, including the effects of thickness. The results of these calculations are shown by the dotted line in figure 4. It is evident that the theory adjusted for thickness effects does provide a better estimation of $C_{h\delta}$ than the linear theory. However, there are still appreciable differences at the lower supersonic Mach numbers.

In figure 5 the values of $C_{h\delta}$ obtained in the present investigation at an angle of attack of 5° are compared with corresponding data from reference 1 and with static data to indicate the effects of frequency. The static data were obtained from tests of a geometrically similar model reported by Boyd and Pfyl in reference 6. In both dynamic investigations the frequency of oscillation was held constant through the tests and, as a result, the reduced frequency k varied with Mach number. At supersonic speeds, the reduced frequency varied from 0.095 at $M = 1.3$ to 0.078 at $M = 1.9$ for the present investigation and from 0.030 to 0.023 for the same Mach number range in the investigation described in reference 1. The theoretical results were calculated for fixed values of k of 0.10 and 0.03. This was done rather than taking into account the change in k present in the experiment, since the theory shows the effect of frequency is small in this range of reduced frequencies.

The prediction of the theory that frequency would have a small effect on $C_{h\delta}$ up to $k = 0.10$ was, in general, borne out by the experimental data at this angle of attack. Good agreement between static and dynamic data is also noted at both subsonic and supersonic speeds.

Damping moments.- Figure 6 shows the variation of aerodynamic damping-moment coefficient with Mach number for oscillation amplitudes of $\pm 1.0^\circ$ and $\pm 2.5^\circ$. It is seen that the effects of angle of attack on the damping-moment coefficient are small for both subsonic and supersonic Mach numbers. In addition, there is a range of Mach numbers for which the damping coefficient is positive or destabilizing. Comparison of the theoretical results with experiment shows a lack of agreement over a large portion of the supersonic speed range investigated. The experimental data indicate, in general, values of $C_{h\delta}$ that are more positive than the theoretical results. Here again the effects of thickness hold a possible explanation for part of the discrepancy between theory and experiment. It has been shown in references 8 and 9 that second-order thickness effects have a small destabilizing influence on the damping moment for harmonically oscillating wings. While the analyses of these two papers are not directly applicable to the determination of $C_{h\delta}$, it is reasonable to assume that a similar destabilizing influence might be found if thickness effects were included in the theoretical determination of this coefficient. It is not likely, however, that the effects of thickness would account for the entire difference between linear theory and experiment since in both references 8 and 9 these effects were found to be small.

It should be noted again that Berman's analysis is based on a control surface having a rectangular plan form rather than the trapezoidal plan form used in the present investigation. It is evident that this fact will account for only a small portion of the discrepancy between theory and experiment since it does not explain the lack of agreement at the higher supersonic Mach numbers where the tip effects should be small.

In figure 7, the values of $C_{h\delta}$ obtained at $\alpha = 10^\circ$ in the present investigation are compared with data from reference 1 to show frequency effects. The theoretical results were again calculated for $k = 0.10$ and 0.03 . At an oscillation amplitude of $\pm 1.0^\circ$ the effect of frequency on $C_{h\delta}$ was small, thus agreeing with the theoretical prediction. However, the data obtained at an amplitude of $\pm 2.5^\circ$ show a destabilizing shift with increasing frequency. The reason for this trend at the higher oscillation amplitude is not known at the present time.

CONCLUSIONS

The results of an experimental investigation of the hinge-moment characteristics of a constant-chord control surface oscillating at high frequency led to the following conclusions:

1. Linear theory provides a reliable guide to the estimation of the trend of the restoring-moment coefficient $C_{h\delta}$ with Mach number for the supersonic speed range of the investigation but overestimates the magnitude of the coefficient. Adjusting the calculated values for second-order thickness effects improves the agreement between theoretical and experimental magnitudes.
2. The experimental values of damping-moment coefficient are, for the most part, more positive than those indicated by the theory and for some conditions can lead to instability of the control surface.
3. The effect of frequency on the restoring-moment coefficient was found to be small, thus agreeing with theoretical predictions. The damping-moment coefficient was similarly insensitive to frequency at an oscillation amplitude of $\pm 1.0^\circ$, but at an amplitude of $\pm 2.5^\circ$ the results showed a destabilizing shift with increasing frequency.

Ames Aeronautical Laboratory
National Advisory Committee for Aeronautics
Moffett Field, Calif., Oct. 24, 1955

APPENDIX A

DESCRIPTION OF TORQUE MOTOR

As pointed out in the body of this paper, the requirement of high frequency of oscillation for this investigation led to the consideration of a torque motor as power for the drive system. Since it is felt that this device has possible application in a variety of dynamic systems where a high-frequency oscillatory torque is desired, a brief description of the design, construction, and calibration of the motor used in this investigation is given.

A schematic diagram of the torque motor is shown in figure 8. The motor is similar in operating principle to that of a polarized relay, consisting of a source of fixed flux distributed equally through the four motor pole pieces and a source of varying flux imposed on the armature. The varying flux polarizes the armature in such a manner that it is attracted by one pair of diagonal poles and repelled by the other, producing a correspondingly varying torque on the armature.

Theory

The theoretical considerations and design equations that follow were obtained from work done by McNicholas in reference 10. It should be pointed out that similar equations along with a design procedure have been developed by Dunn in reference 11. McNicholas has shown that the torque on the armature can be written in the form

$$T = K_1 \phi_f \phi_v \quad (A1)$$

where

T torque

K_1 constant determined by the geometry of the motor

ϕ_f fixed (permanent) flux

ϕ_v varying (armature) flux

If the varying flux is assumed to be below the saturation level then

$$\phi_v = K_2 i_v \quad (A2)$$

where

K_2 constant depending on the magnetic properties of the armature flux path

i_v armature current

By substitution of this expression for ϕ_v in equation (A1)

$$\begin{aligned} T &= K_1 K_2 \phi_v i_v \\ &= K_m i_v \end{aligned} \tag{A3}$$

where K_m is defined as the motor constant.

The assumptions inherent in the formulation of equations (A2) and (A3) are the following: (a) no fixed flux in the armature, which can be approximated if the movement of the armature is small with respect to the size of the air gap, and (b) the reluctance of the path of the varying flux is constant, which is possible if the armature flux is eliminated from the excitation yoke. Equation (A3) shows that, within the limits of these assumptions, the torque output of the motor is a linear function of the armature current.

Design Considerations and Construction

The primary requirements dictating the design of the torque motor for this investigation were torque required, amplitude of oscillation, and space limitations. The magnetic properties of the motor were calculated in a manner similar to those of reference 10 while the physical dimensions were established by size and inertia limitations and torque requirements.

There were two points where the design of the present motor departed from those described in references 10 and 11. The motors described in those papers used permanent magnets to provide the fixed flux for motor excitation in order to keep the motor as simple as possible. In the wind-tunnel installation, however, it was felt that the additional fixed flux attainable through the use of a field winding would offset the added complication of a field current power supply. For this reason, a field winding was used to supply the fixed flux for motor excitation. The other modification consisted of the addition of a shorted turn of copper at each end of the excitation yoke to increase the reluctance of the yoke to the varying flux.

The motor constructed for this investigation consisted of motor pole pieces and armature made of laminations of 29-gage transformer steel and an excitation yoke made of solid soft iron. The excitation field winding was made in two coils wound from number 30 magnet wire, having 4600 turns each and connected in parallel, flux adding. The two armature coils were also wound from number 30 magnet wire and had 1100 turns each. They were connected in series, flux adding. The motor pole pieces, excitation yoke, and coils were supported by brass side plates. A photograph of the motor is shown in figure 9.

Calibration

The torque versus current characteristic of the motor is shown in figure 10. To obtain the data for this curve, the armature was mounted in ball bearings and was supported in a centered position between the pole pieces. Torque was then applied to the armature shaft by a series of weights hung on a lever arm. The current required to rotate the armature from the supported position for various load torques was then recorded. The field current was held constant for the calibration. Figure 10 shows that a linear variation of torque with armature current was achieved up to the maximum value of armature current impressed on the motor.

One other quantity remained to be evaluated in the static calibration. When the armature is deflected from a position midway between the pole pieces, a torque due to the redistribution of the permanent flux is produced which tends to increase the deflection. This torque is referred to as an "anti-spring torque" by McNicholas. To determine the variation of this torque with armature deflection angle, the armature was loaded with a fixed torque and supported against this torque at several angles from the neutral position. The current required to overcome the load torque was then recorded. The change in current required as the deflection angle increased has been plotted as a function of deflection angle in figure 11. It can be seen that the anti-spring torque is a linear function of δ above a deflection angle of $1/2^\circ$. The reason for the nonlinear variation from $\delta = 0^\circ$ to $\delta = 1/2^\circ$ is not known at the present time. It should be noted that since the anti-spring torque was approximately a linear function of deflection, its effect would simply be to decrease the spring constant of the mechanical system by a small amount.

REFERENCES

1. Reese, David E., Jr.: An Experimental Investigation at Subsonic and Supersonic Speeds of the Torsional Damping Characteristics of a Constant-Chord Control Surface on an Aspect Ratio 2 Triangular Wing. NACA RM A53D27, 1953.
2. Frick, Charles W., and Olsen, Robert N.: Flow Studies in the Asymmetrical Adjustable Nozzle of the Ames 6- by 6-Foot Supersonic Wind Tunnel. NACA RM A9E24, 1949.
3. Runyan, Harry L., Woolston, Donald S., and Rainey, A. Gerald: Theoretical and Experimental Investigation of the Effect of Tunnel Walls on the Forces on an Oscillating Airfoil in Two-Dimensional Subsonic Compressible Flow. NACA TN 3416, 1955.
4. Woolston, Donald S., and Runyan, Harry L.: Some Considerations on the Air Forces on a Wing Oscillating Between Two Walls for Subsonic Compressible Flow. IAS Preprint 446, Jan. 25, 1954.
5. Nelson, Herbert C., Rainey, Ruby A., and Watkins, Charles E.: Lift and Moment Coefficients Expanded to the Seventh Power of Frequency for Oscillating Rectangular Wings in Supersonic Flow and Applied to a Specific Flutter Problem. NACA TN 3076, 1954.
6. Boyd, John W., and Pfyl, Frank A.: Experimental Investigation of Aerodynamically Balanced Trailing-Edge Control Surfaces on an Aspect Ratio 2 Triangular Wing at Subsonic and Supersonic Speeds. NACA RM A52L04, 1953.
7. Staff of the Ames 1- by 3-Foot Supersonic Wind-Tunnel Section: Notes and Tables for Use in the Analysis of Supersonic Flow. NACA TN 1428, 1947.
8. Tobak, Murray: Damping In Pitch of Low-Aspect-Ratio Wings at Subsonic and Supersonic Speeds. NACA RM A52L04a, 1953.
9. Van Dyke, Milton D.: Supersonic Flow Past Oscillating Airfoils Including Nonlinear Thickness Effects. NACA TN 2982, 1953.
10. McNicholas, Robert Joseph: Theoretical and Experimental Study of a New, Small, High-Speed Linear Torque Motor. Bumblebee Rep. No. 183, Johns Hopkins Univ., Appl. Phys. Lab., Silver Spring, Md., July 1952.
11. Dunn, John F., Jr.: A Study of Permanent-Magnet Torque Motors. Res. Memo. RM 6387-5, MIT, Dynamic Analysis and Control Lab., Apr. 30, 1954.

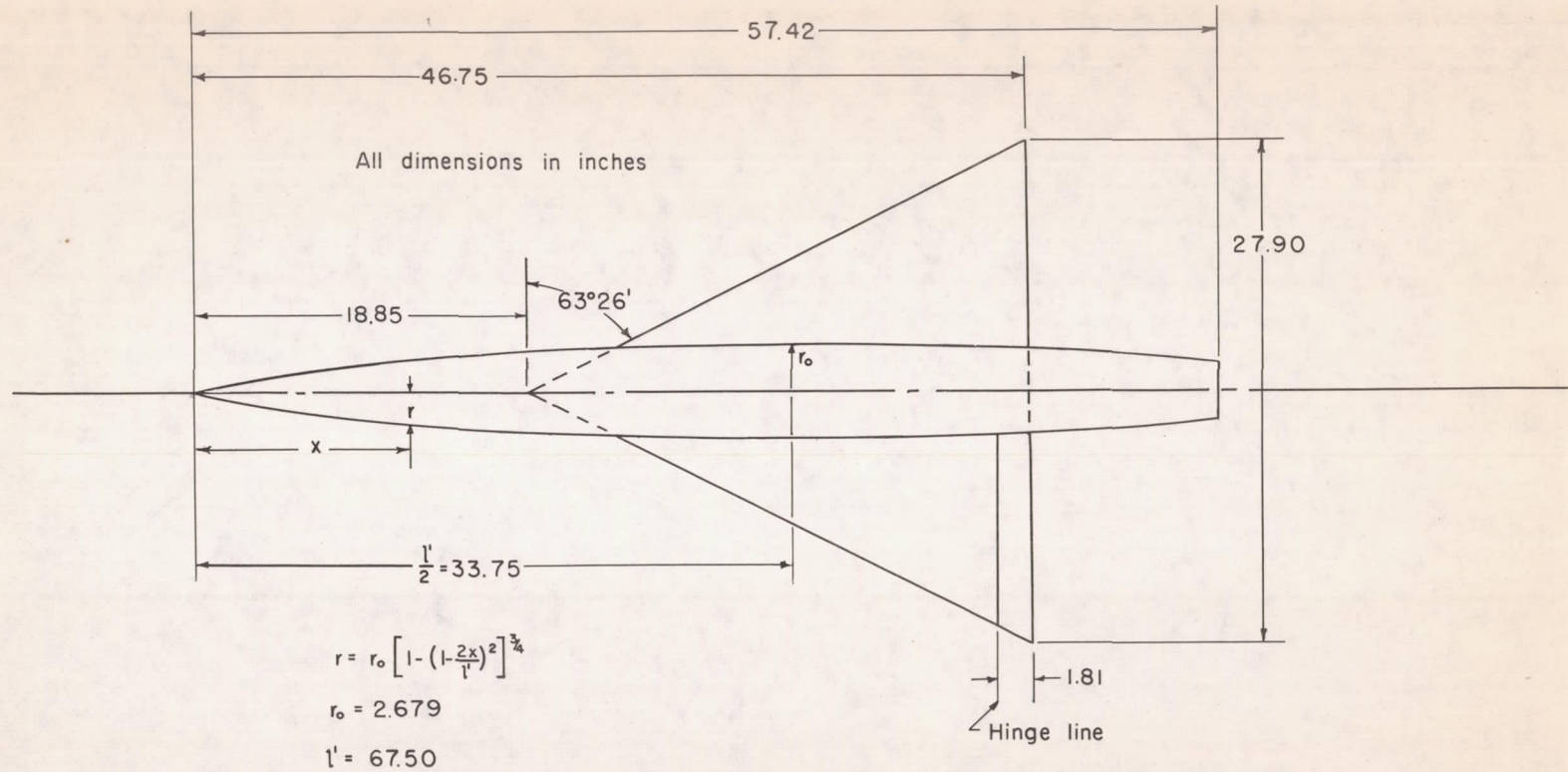
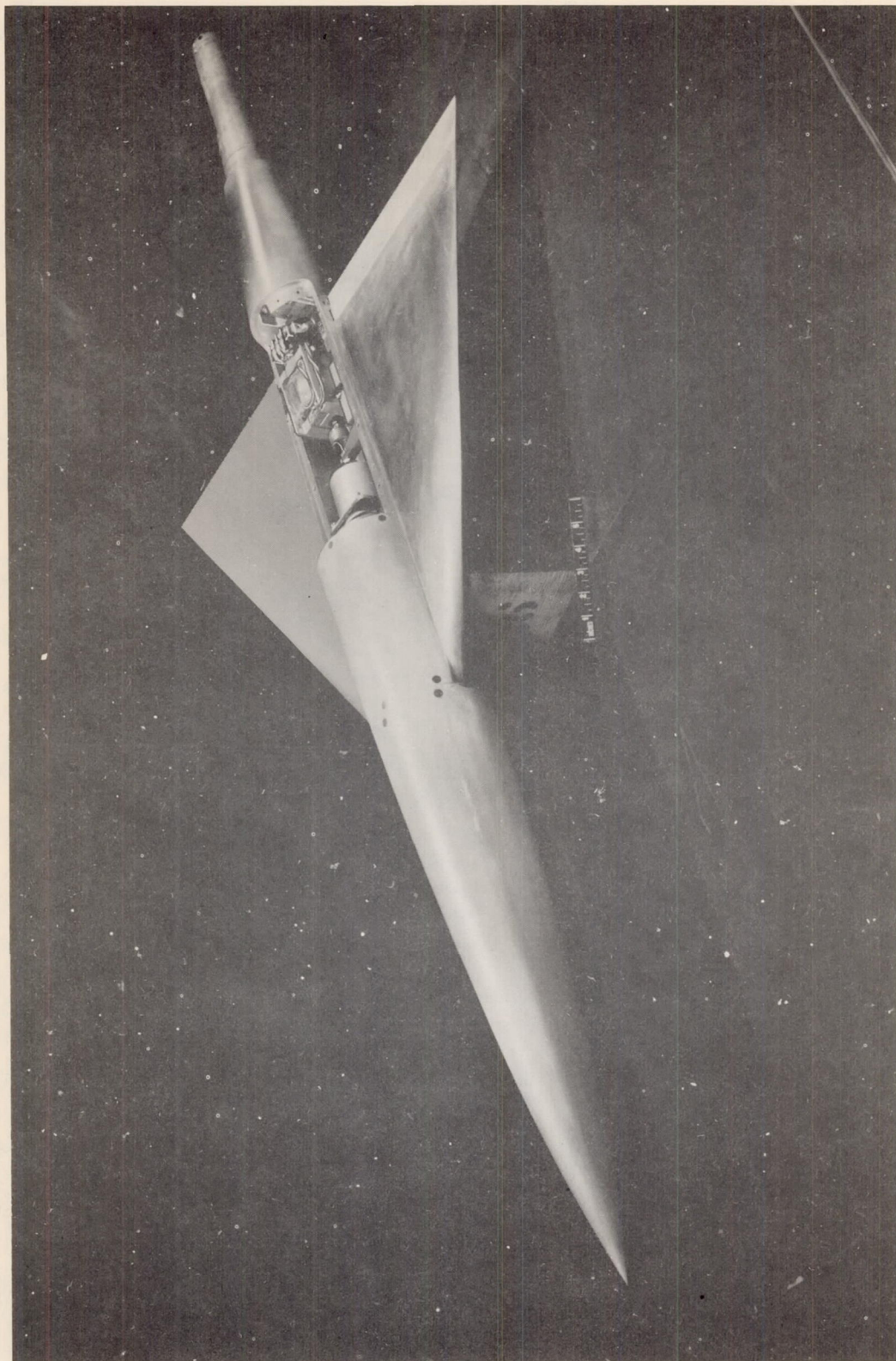


Figure 1.-Sketch of model.



A-19773.1

Figure 2.- Photograph of model with cover removed.

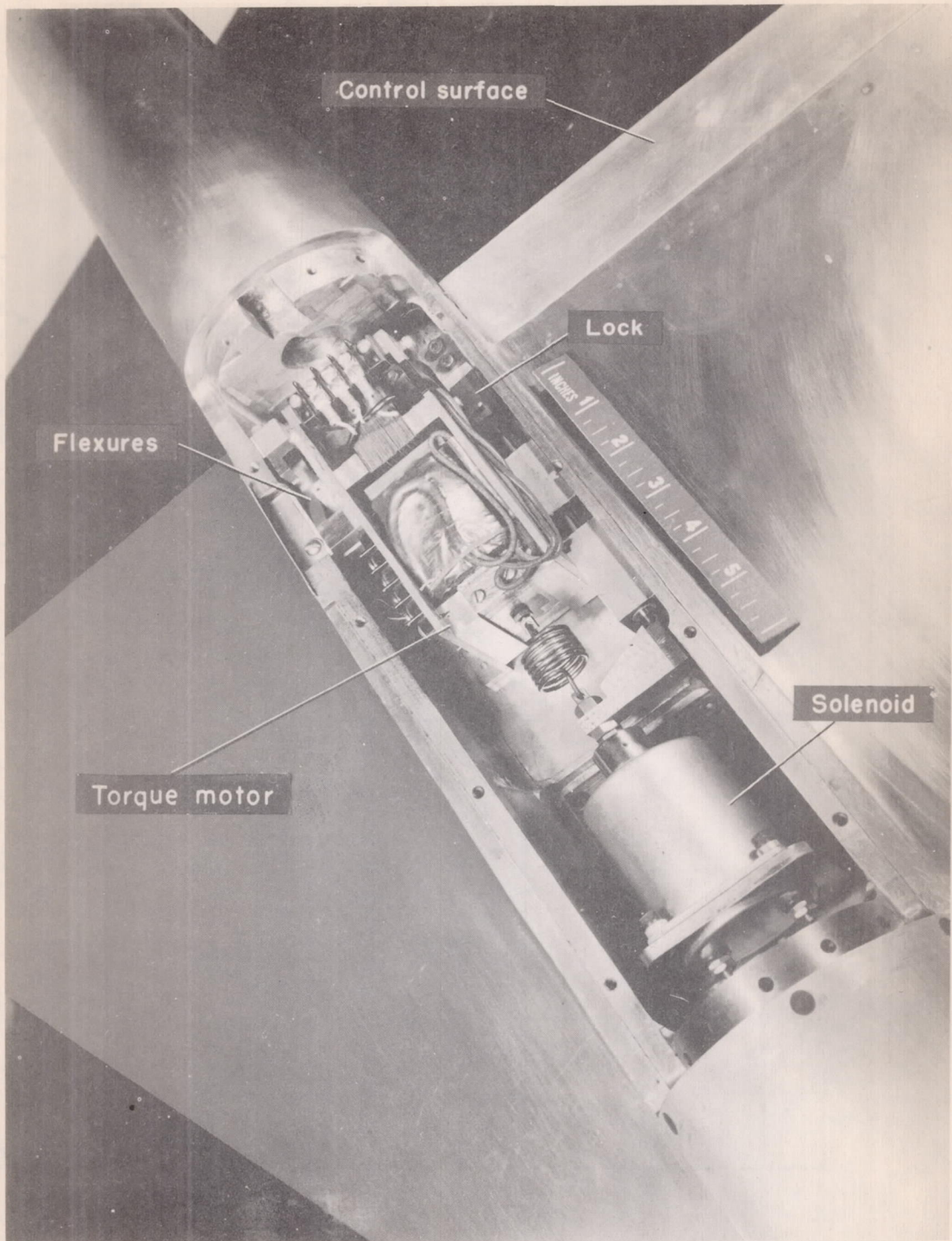


Figure 3.- View of model drive system.

A-19774.2

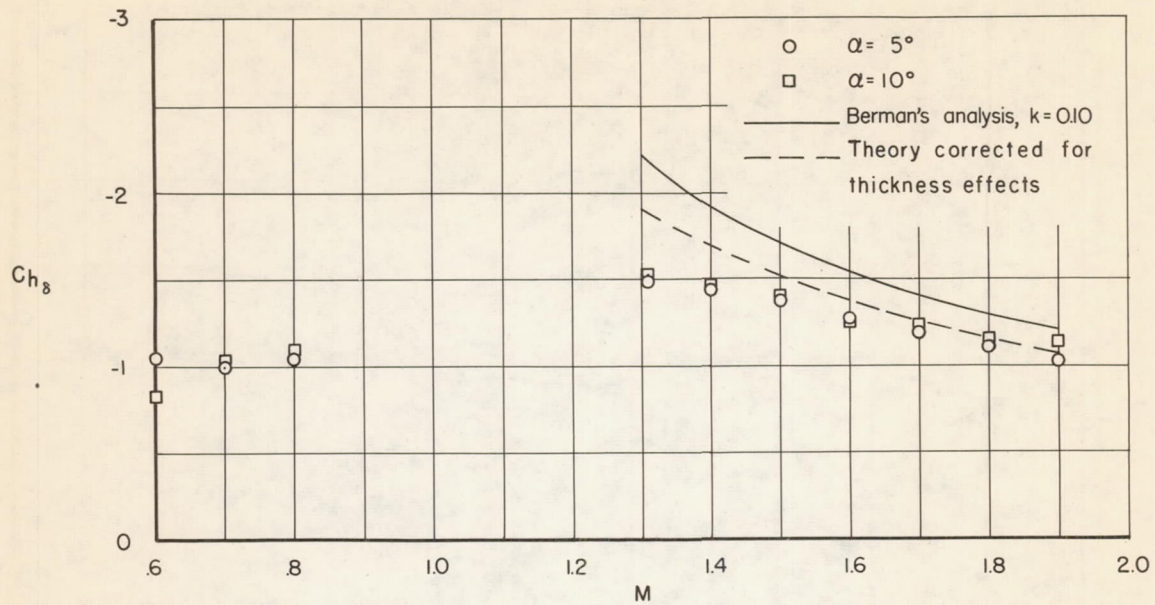


Figure 4. - The effect of angle of attack on the aerodynamic restoring-moment coefficient.

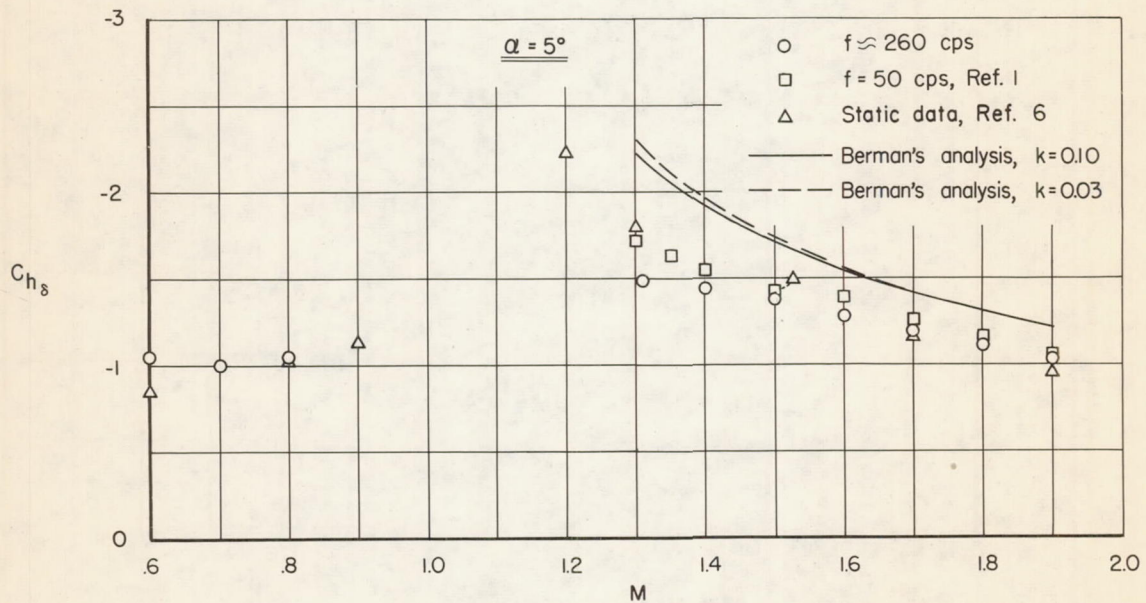


Figure 5. - The effect of frequency on the aerodynamic restoring-moment coefficient.

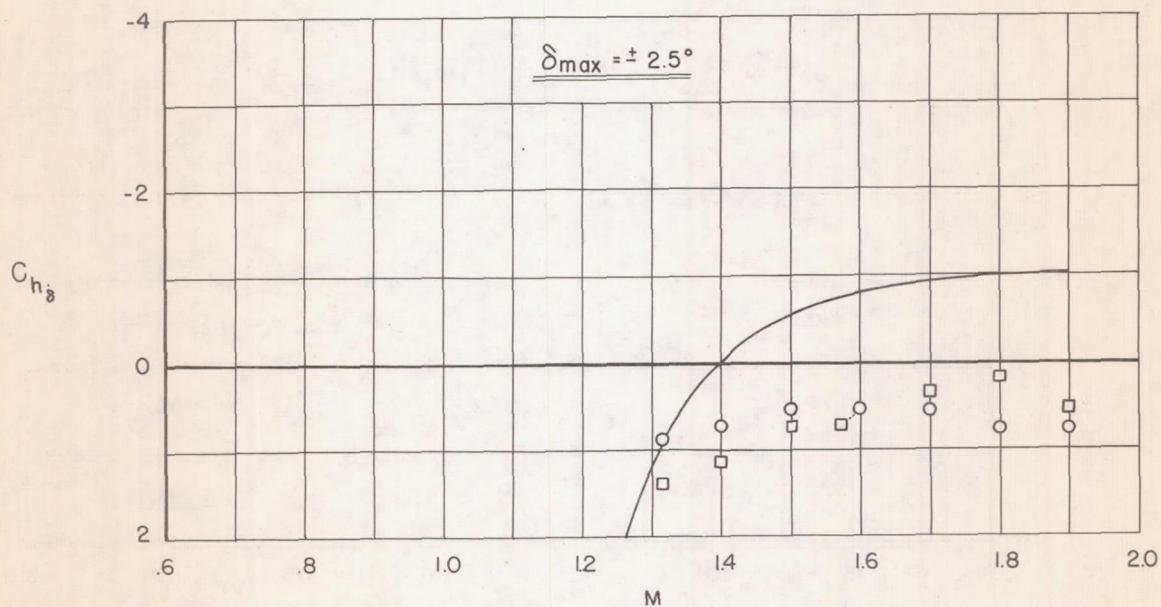
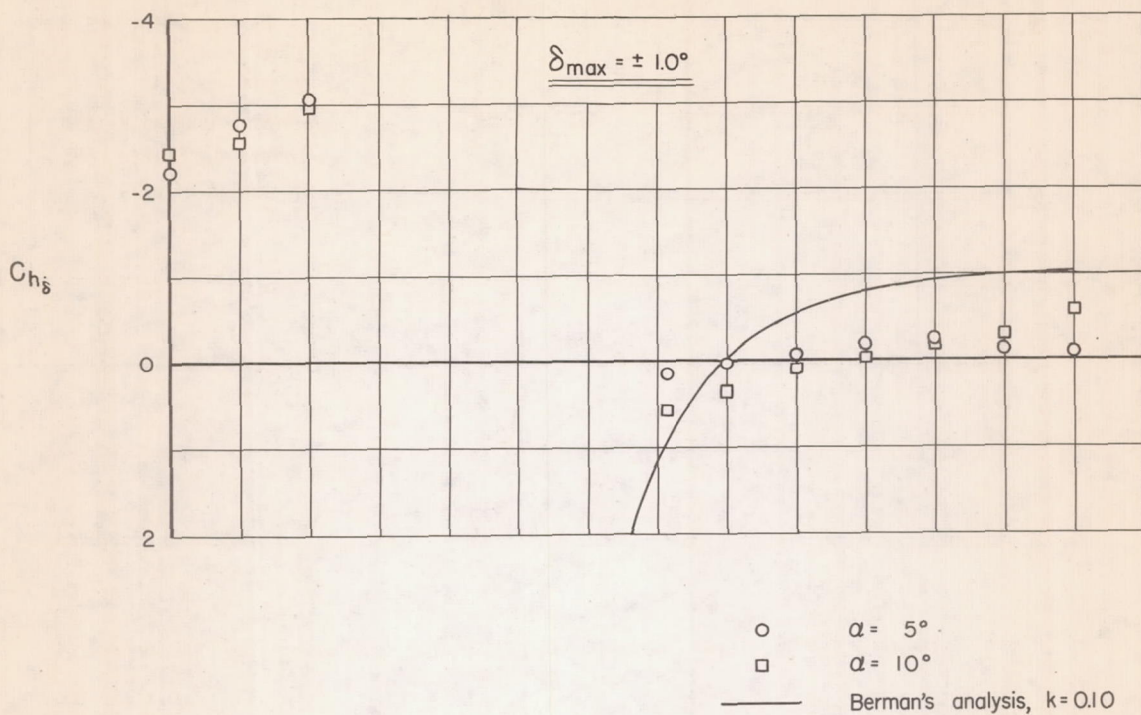
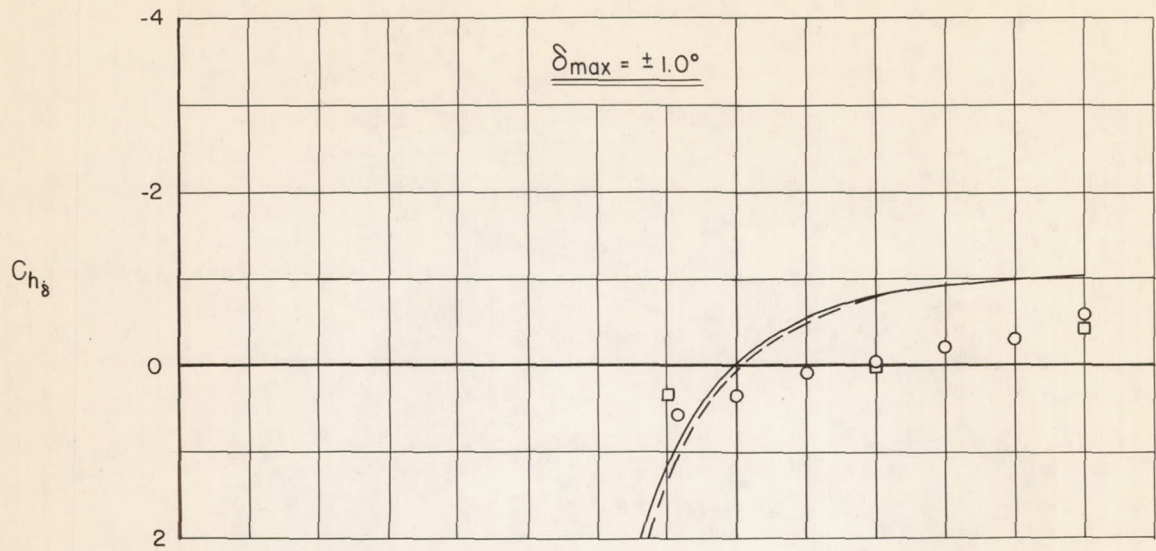


Figure 6. - The effect of angle of attack on the aerodynamic damping-moment coefficient.



- $f \approx 260$ cps
- $f = 50$ cps, Ref. 1
- Berman's analysis, $k = 0.10$
- - - Berman's analysis, $k = 0.03$

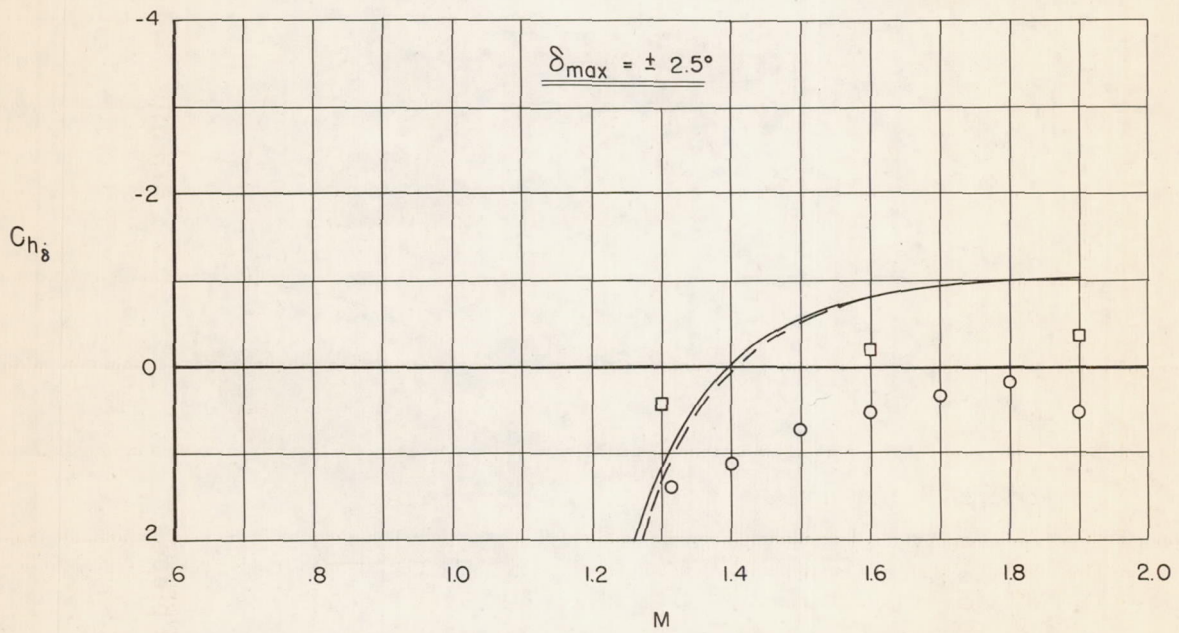
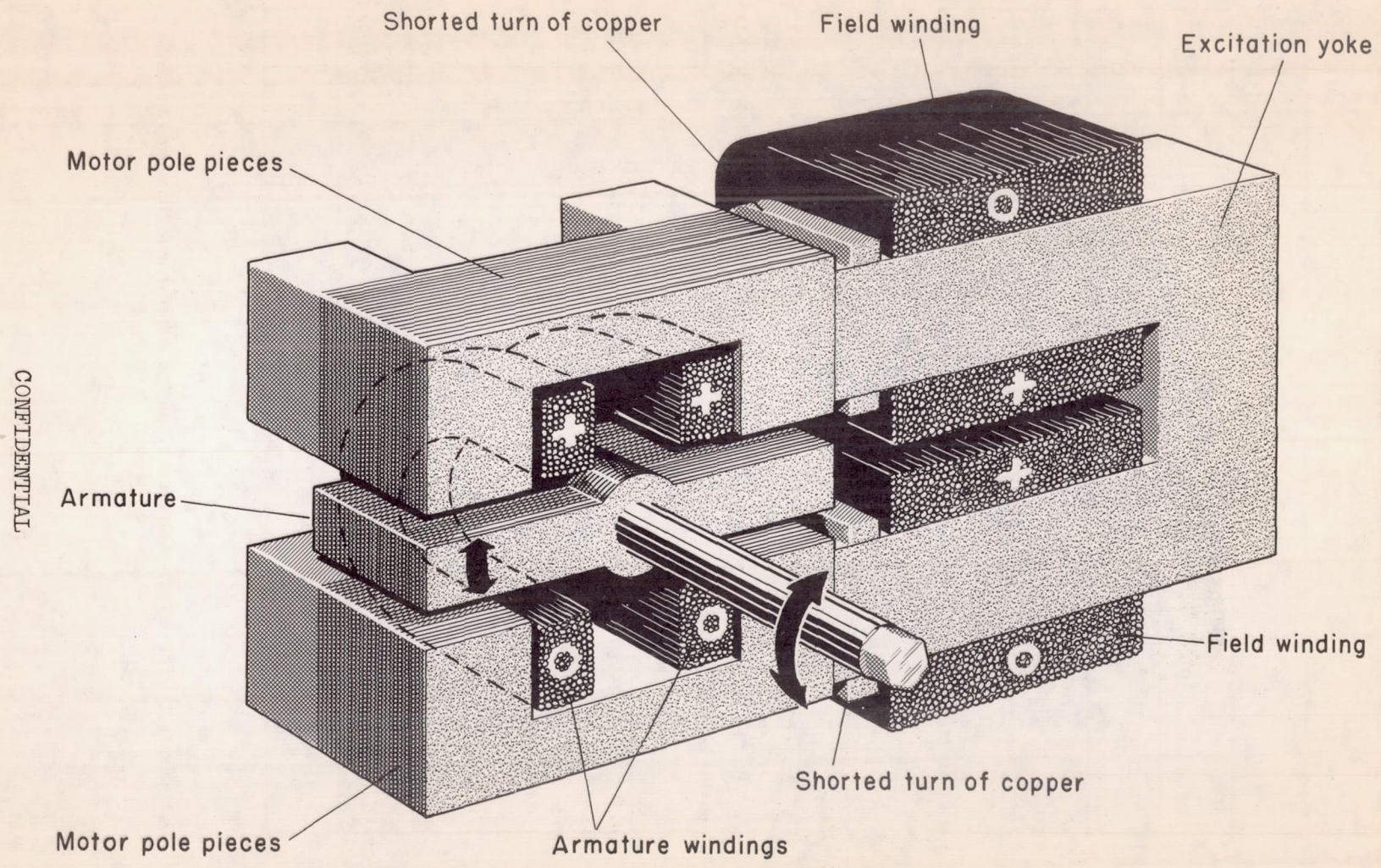
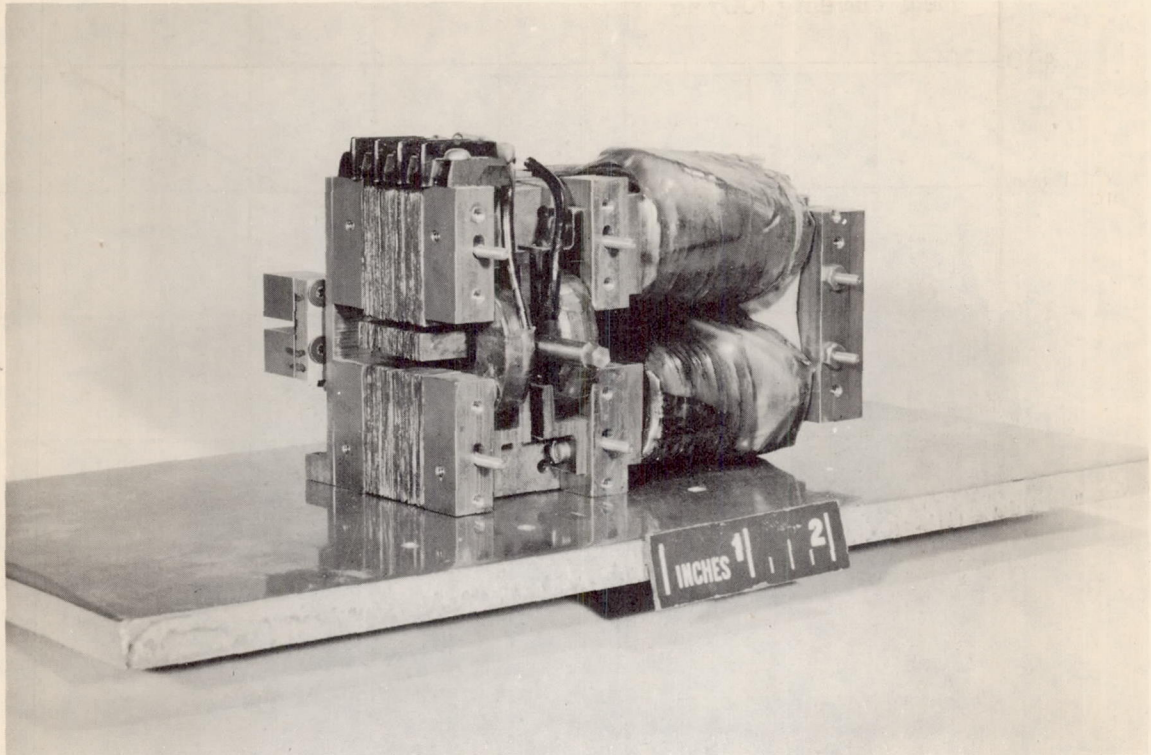


Figure 7 - The effect of frequency on the aerodynamic damping-moment coefficient, $\alpha = 10^\circ$.



CONFIDENTIAL

Figure 8.- Schematic diagram of torque motor.



A-19776

Figure 9.- Photograph of torque motor with side plate removed.

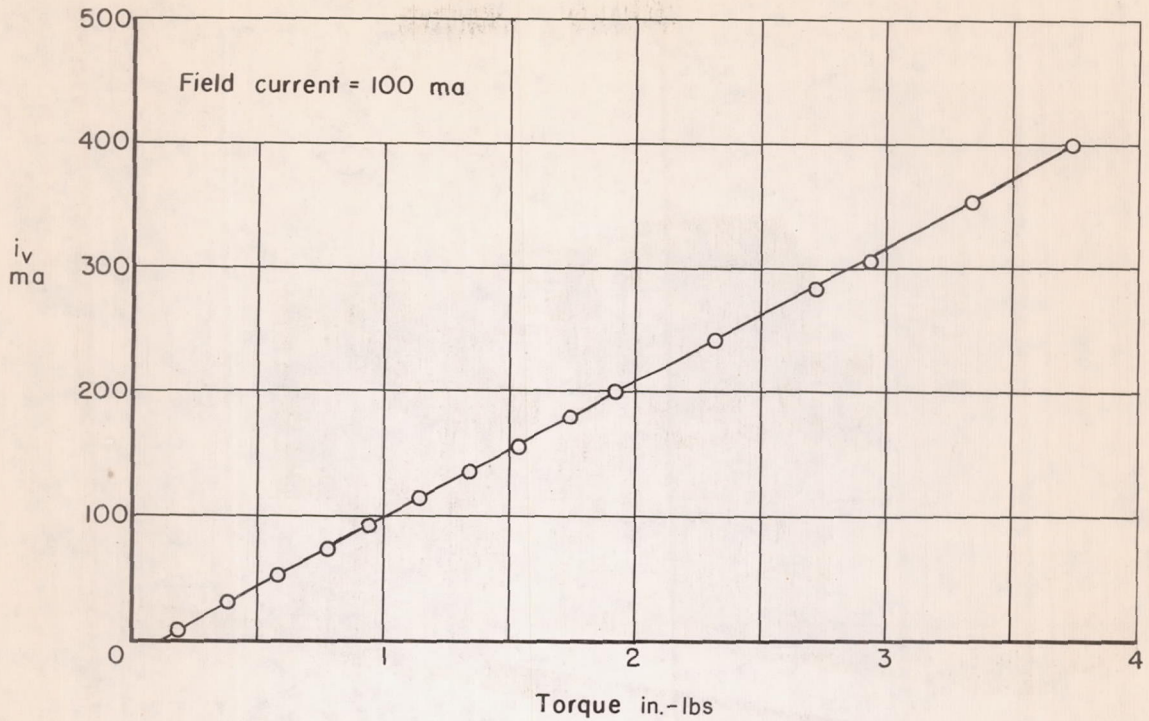


Figure 10. - Static torque calibration of motor.

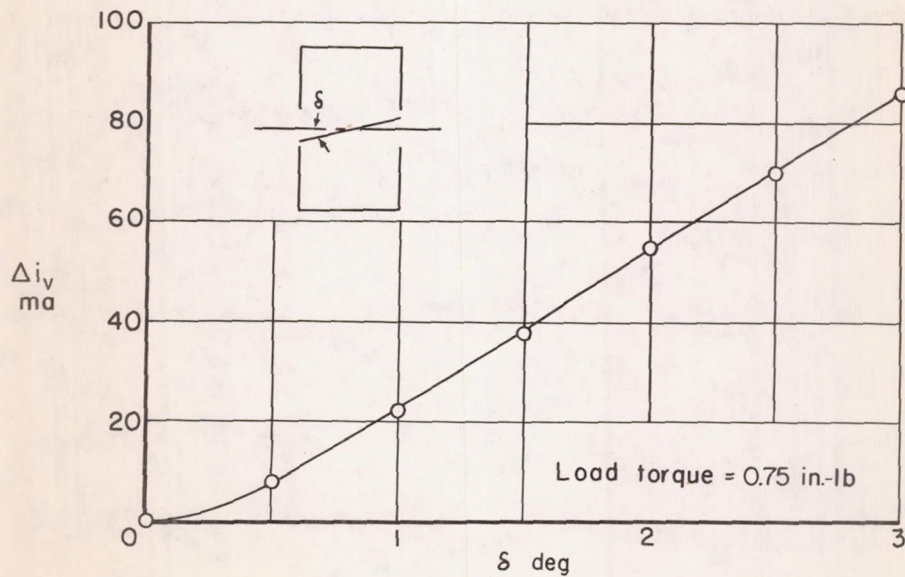
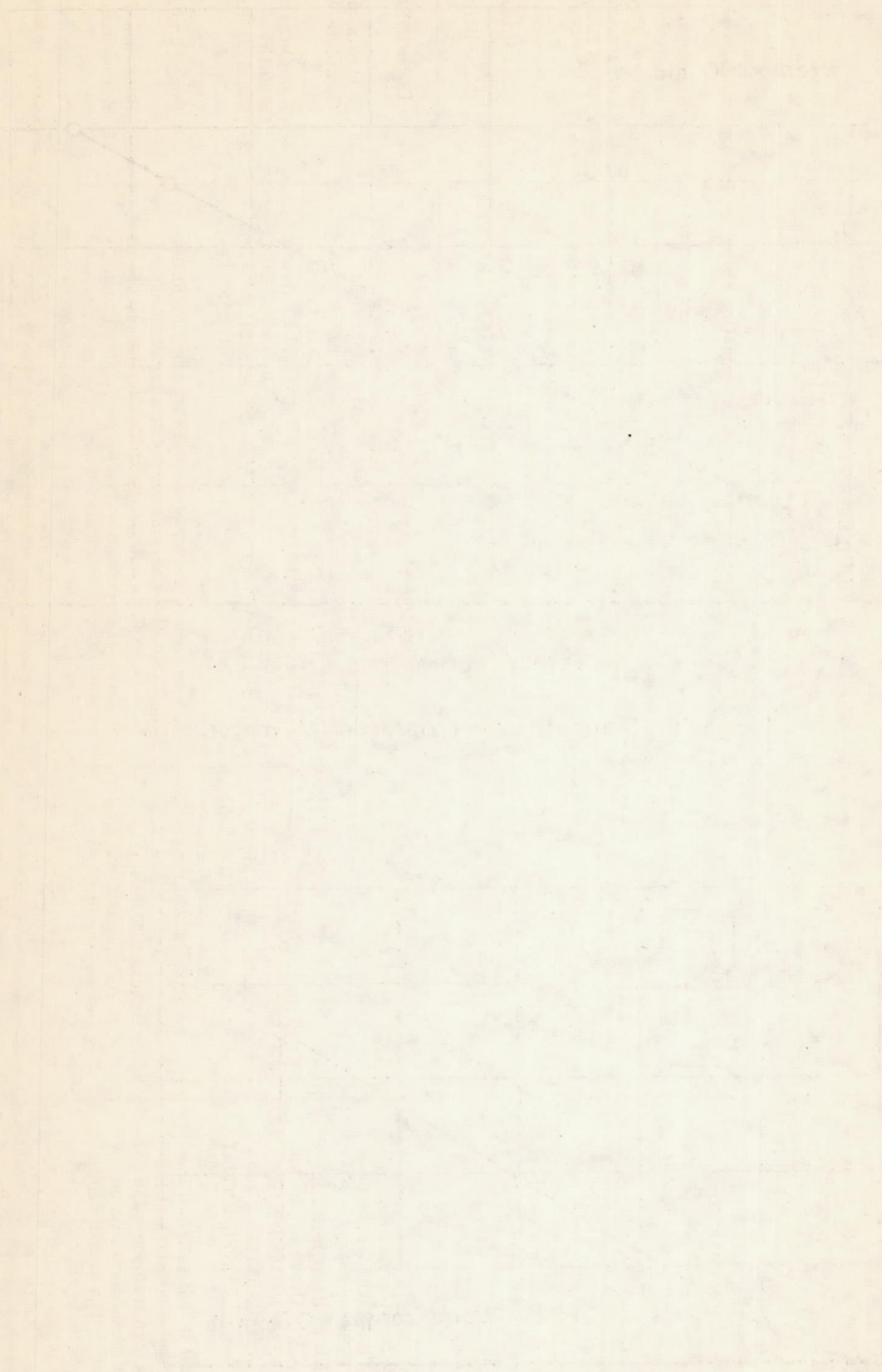
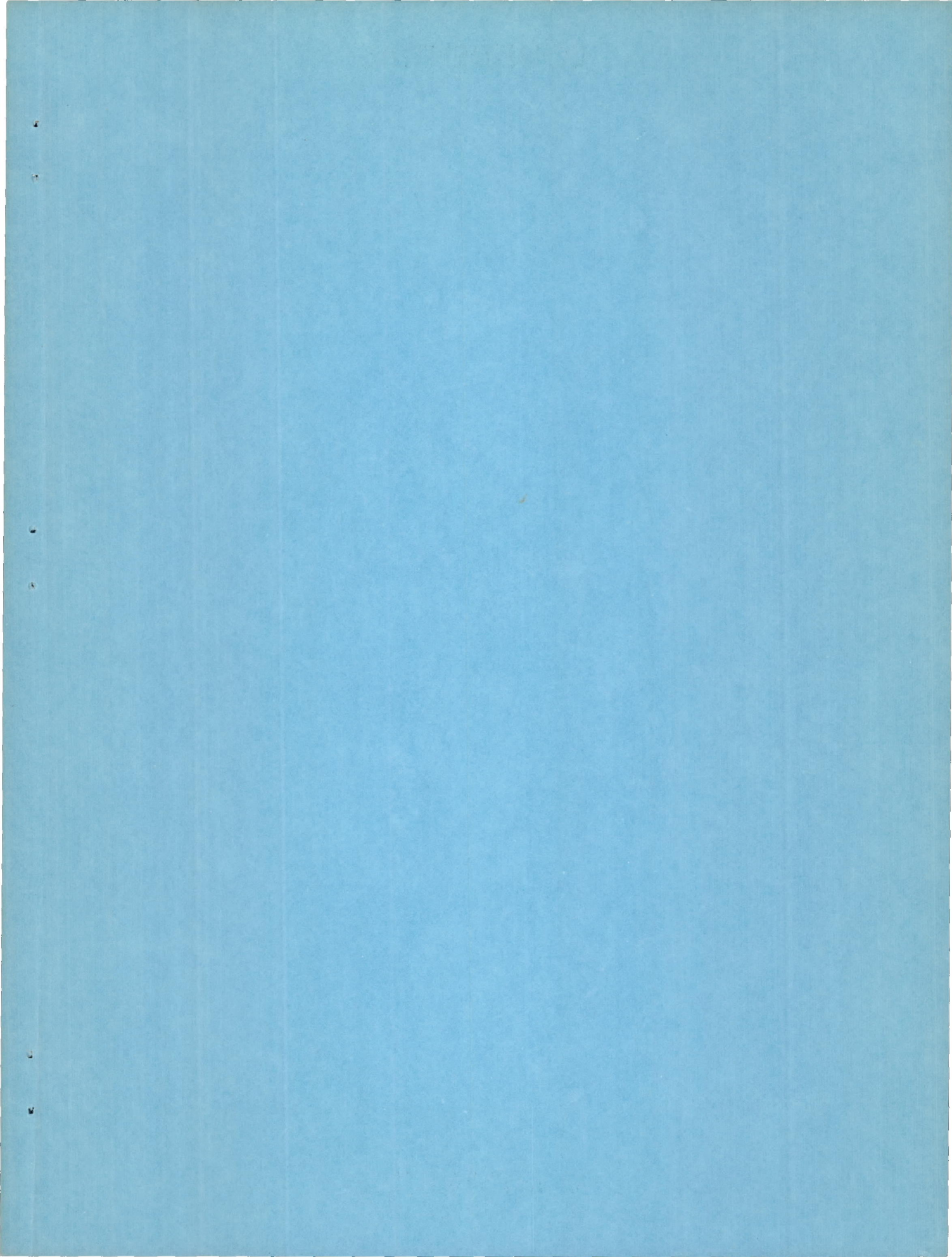


Figure 11. - Variation of armature current with deflection angle for a constant armature torque.





CONFIDENTIAL
UNCLASSIFIED

UNCLASSIFIED
CONFIDENTIAL